HHS Public Access

Author manuscript

Circ Res. Author manuscript; available in PMC 2021 January 17.

Published in final edited form as:

Circ Res. 2020 January 17; 126(2): 232–242. doi:10.1161/CIRCRESAHA.119.315531.

Loss of Endothelial FTO Antagonizes Obesity-Induced Metabolic and Vascular Dysfunction

Nenja Krüger[1,2], **Lauren A Biwer**[1,3], **Miranda E Good**[1], **Claire A. Ruddiman**[1,4], **Abigail G. Wolpe**[1,5], **Leon J DeLalio**[1,4], **Sara Murphy**[1], **Edgar H. Macal Jr**[1], **Louis Ragolia**[6], **Vlad Serbulea**[1,3], **Angela K Best**[1], **Norbert Leitinger**[1,4], **Thurl E. Harris**[4], **Swapnil K Sonkusare**[1,3], **Axel Gödecke**[7], **Brant E Isakson**[1,3]

[1]Robert M Berne Cardiovascular Research Center, University of Virginia School of Medicine;

[2]Institute of Animal Developmental and Molecular Biology, Heinrich Heine University Düsseldorf, Germany;

[3]Department of Molecular Physiology and Biophysics, University of Virginia School of Medicine, PO Box 801394, Charlottesville, VA 22908 USA;

[4]Department of Pharmacology, University of Virginia School of Medicine;

[5]Department of Cell Biology, University of Virginia School of Medicine;

[6]Department of Biomedical Research, NYU Winthrop University Hospital, NYU Long Island School of Medicine;

[7]Institute of Cardiovascular Physiology, Heinrich Heine University Düsseldorf, Germany.

Abstract

Rationale: Increasing prevalence of obesity and its associated risk with cardiovascular diseases demands a better understanding of the contribution of different cell types within this complex disease for developing new treatment options. Previous studies could prove a fundamental role of the *Fat mass and obesity associated gene* (*Fto*) within obesity; however, its functional role within different cell types is less understood.

Objectives: We identify endothelial FTO as a previously unknown central regulator of both obesity-induced metabolic and vascular alterations.

Methods and Results: We generated endothelial *Fto*-deficient mice and analyzed the impact of obesity on those mice. While the loss of endothelial FTO did not influence the development of obesity and dyslipidemia, it protected mice from high fat diet (HFD)- induced glucose intolerance and insulin resistance by increasing AKT phosphorylation in endothelial cells and skeletal muscle. Furthermore, loss of endothelial FTO prevented the development of obesity-induced hypertension by preserving myogenic tone in resistance arteries. In *Fto*-deficient arteries, microarray analysis identified upregulation of *Lipocalin-type prostaglandin D synthase (L-Pgds)* with significant

Address correspondence to: Dr. Brant E Isakson, Robert M Berne Cardiovascular Research Center, University of Virginia School of Medicine, Tel: 434-924-2093, brant@virginia.edu.

DISCLOSURES

The authors declare no conflict of interests.

increases in prostaglandin D_2 (PGD_2) levels. Blockade of PGD_2-synthesis inhibited the myogenic tone protection in resistance arteries of endothelial *Fto*-deficient mice on HFD; conversely, direct addition of PGD_2 rescued myogenic tone in HFD-fed control mice. Myogenic tone was increased in obese human arteries with FTO inhibitors or PGD_2 application.

Conclusion: These data identify endothelial FTO as a previously unknown regulator in the development of obesity-induced metabolic and vascular changes, which is independent of its known function in regulation of obesity.

Graphical Abstract

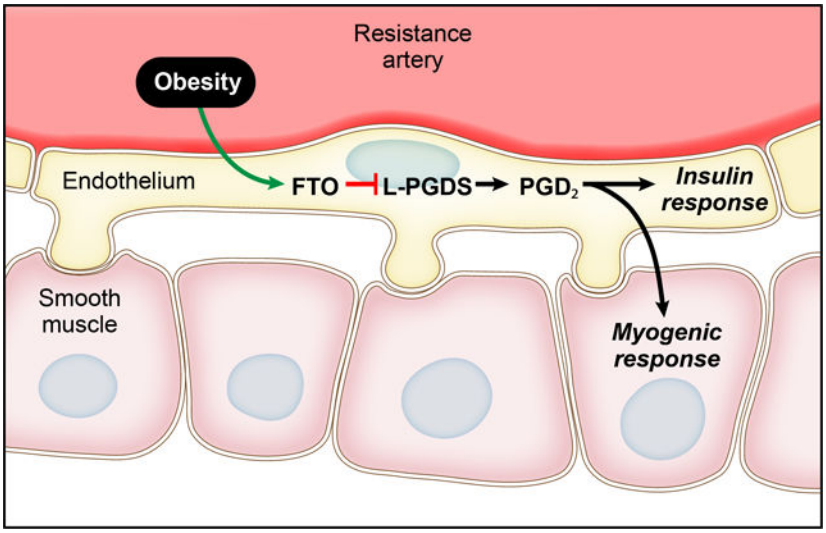

Abstract

The present study demonstrates that deletion of FTO from endothelium in mice has no effect on the ability of mice to gain weight in response to high fat diet (i.e., they still become obese). However, obese mice lacking endothelial FTO have marked improvements in insulin sensitivity, myogenic tone of resistance arteries, and blood pressure. These effects are mediated by altered expression of L-PGDS, the main enzyme used to make PGD_2. In obese human arteries, inhibition of FTO or application of PGD_2 also increased myogenic tone, similar to that seen in mouse arteries. This work identifies a novel pathway regulating the vascular response to obesity.

Keywords

Fto; endothelial cell; obesity; PGD_2; hypertension; type 2 diabetes mellitus

Subject Terms:

Vascular Biology; Vascular Disease

INTRODUCTION

The worldwide incidence of obesity is dramatically increasing and presents health care systems with high economic burdens through accelerated development of cardiovascular

diseases (CVDs)[1]. This impact on cardiovascular health is primarily due to the development of hyperglycemia, insulin resistance, and dyslipidemia[2–4]. Furthermore, obesity alters vascular homeostasis, which favors the ontogeny of pathologic hypertension, further increasing CVD risk and mortality[5, 6].

Previous genome-wide association studies (GWAS) in human attempting to identify candidate genes that influence obesity proved that different single nucleotide polymorphisms (SNP) within the *Fat mass and obesity associated* gene *(FTO)* highly correlate with increased risk of obesity[7]. Although there are controversial reports, if those SNPs correlate with FTO or Iroquois homeobox 3 (IRX3) expression in human tissues, murine studies proved a causative role of FTO within *Fto*-deficient mice being protected against the development of obesity[8–10]. Further, metabolic analysis in Leptin-deficient mice showed a functional role of FTO in glucose tolerance additionally linking FTO to obesity-induced metabolic alterations[11]. Although FTO is known to be a N6-methyladenosine RNA demethylase, important cell types and molecular mechanism leading to obesity-induced metabolic alterations by loss of FTO remained largely unknown[12].

Within obesity-induced alterations, endothelial cells (EC) have a central role because of their unique localization. As EC are the cell type in contact with the flowing blood, they represent a barrier for metabolites to the following organs. Previous studies proved that obesity decreases AKT phosphorylation in EC, which impaired glucose and insulin tolerance by decreasing interstitial insulin concentration and glucose uptake of skeletal muscle[13]. In addition to their metabolic role, EC significantly impact peripheral resistance via tight heterocellular communication with adjacent smooth muscle cells (SMC), especially in resistance arteries, which are the main contributor to vascular resistance[14]. In those arteries, the EC can influence myogenic tone via endothelial derived hyperpolarization (EDH), release of prostaglandins and nitric oxide. While EDH depends on the activation of endothelial small and intermediate Ca^{2+} -activated potassium channel (IK_{Ca}, SK_{Ca}) and inward rectifier potassium channels (K_{ir}) leading to EC hyperpolarization and subsequent spread of hyperpolarization to adjacent SMC, prostaglandins activate G-protein coupled receptors on SMC to induce hyperpolarization, and nitric oxide activates cGMP to directly dilate SMC[15–17]. In this way, EC have a direct impact on peripheral resistance and blood pressure.

Because EC are a central cell type in obesity-induced metabolic and vascular changes, we wanted to analyze the functional role of endothelial FTO in this process[13, 18]. Therefore, we generated EC-specific *Fto* deficient mice. Surprisingly, we identified a direct influence of endothelial FTO on the development of obesity-induced insulin resistance, hyperglycemia, hypertension and vascular resistance, without influencing the development of obesity. Further, we could verify the functional role of FTO in regulation of vascular resistance in human obese arteries. These data suggest that FTO has an essential metabolic and vascular effect mediated in the endothelium, which is independent of the gene's role in obesity.

METHODS

Detailed methods can be found in the Online Methods section. The data that support the findings of this study are available from the corresponding author on reasonable request.

Animals.

Male CDH5 CreER^{T2} *Fto*$^{flox/flox}$ mice were either injected with vehicle (EC *Fto*$^{fl/fl}$) or tamoxifen to induce knockout of endothelial FTO (EC *Fto*$^{\Delta/\Delta}$). At 8 weeks, mice were either kept on normal chow or were placed on a 60% high fat diet (BioServ, F3282) for 12 weeks to induce obesity. *L-Pgds*$^{-/-}$ mice were generated as described[19].

Radiotelemetric blood pressure measurement.

Catheters were implanted in the right carotid artery under isoflurane anesthesia as previously described[20]. After a recovery period of 7 days, blood pressure was measured for 7 days and mean arterial pressure calculated.

Pressure myograph analysis.

Murine third order mesenteric arteries and resistance arteries from human adipose tissue were isolated, surrounding tissue removed, cannulated on glass pipettes and pressurized at 80 mmHg until myogenic tone developed, as previously described[21].

Metabolic parameters.

In vivo insulin stimulation, insulin tolerance test and glucose tolerance test were performed as described[22]. SiRNA-transfected human aortic endothelial cells (HAoEC) were subjected to mitochondrial stress tests via seahorse assays as previously described[23].

Quantification and statistical analysis.

Represented data are mean ± SEM (Note: For datapoints, where SEM was too small to be visualized, exact SEM values are reported in Online Table I). Power analysis for each group was determined as described[24]. For statistical data analysis,Graph Pad Prism 7 software was used. To analyze normal distribution of data, Shapiro-Wilk test was performed and revealed normal distribution of all data (see Online Table II for exact p-values). Therefore, if groups of two were analyzed, unpaired t-test was performed. If groups were >2, one-way ANOVA following Tukey's post-hoc test was performed (e.g., insulin tolerance tests). Two-way ANOVA with Tukey's post-hoc was used for multiple comparisons. No experiment-wide multiple test correction was applied. For all experiments, a p-value <0.05 was defined as significant.

RESULTS

Loss of endothelial FTO does not influence the development of obesity.

Because the *Fto* gene has been linked to obesity, and the cardiovascular system and metabolic indices are intimately linked, we first sought to determine if FTO protein changed in obese conditions[8, 11, 25]. Mice were either fed normal chow (NC) or a high fat diet (HFD) for 12 weeks to induce obesity and the FTO protein was analyzed in adipose and third order

mesenteric arteries (where total peripheral resistance can be tightly regulated). In both adipose and mesenteric arteries FTO protein was increased, however it was statistically significant in mesenteric arteries (Figure 1A). In situ hybridization revealed *Fto* mRNA in both smooth muscle and endothelium (Online Figure I). Because of the key role of endothelium in metabolic disease, we decided to focus on the functional role of endothelial FTO in obesity and obesity-induced metabolic and vascular changes[13, 18, 26]. To do this, tamoxifen-inducible EC-specific *Fto*-deficient mice were generated (EC $Fto^{\Delta/\Delta}$; Figure 1B). We verified successful cre-mediated recombination of the *Fto* locus in ECs of EC $Fto^{\Delta/\Delta}$ mice by analyzing genomic DNA using PCR (band size approx. 700 bp; Figure 1C). To further verify the successful knockout of endothelial FTO protein, third order mesenteric arteries were immunostained using an anti-FTO antibody demonstrating the loss of FTO protein in EC of EC $Fto^{\Delta/\Delta}$ mice (Figure 1D).

Next, 8 week old EC $Fto^{fl/fl}$ and EC $Fto^{\Delta/\Delta}$ mice were either fed NC or a HFD for 12 weeks to induce obesity (Figure 1E). There was no change in inflammation status of adipose tissue in these mice (Online Figure II). In addition, analysis of body weight gain over time and body weight at 20 weeks (Figure 1F; Online Figure III) revealed that loss of endothelial FTO did not influence body weight in both NC-fed and HFD-fed mice. The epigonadal fat mass (Figure 1G) was also not different between EC $Fto^{fl/fl}$ and EC $Fto^{\Delta/\Delta}$ mice after both NC and HFD feeding (NC: 0.52 vs. 0.66 g; HFD: 2.9 vs. 2.8 g, respectively). Further analysis of body length (Online Figure III) revealed no differences between EC $Fto^{fl/fl}$ and EC $Fto^{\Delta/\Delta}$ mice in both NC-fed and HFD-fed mice. Analysis of weight gain over time, body weight, epigonadal fat mass and body length revealed no tamoxifen-dependent effects (Online Figure III). Last, we could detect no change in IRX3 protein in mesenteric arteries from either EC $Fto^{fl/fl}$ and EC $Fto^{\Delta/\Delta}$ mice (Online Figure III). Thus, although there is in an increase in FTO protein in mesenteric arteries on a high fat diet, FTO, at least in endothelium, does not appear to influence the capacity to regulate obesity.

Loss of endothelial FTO antagonizes obesity-induced metabolic changes.

To investigate if endothelial FTO is important in the development of obesity-induced dyslipidemia and insulin resistance, blood lipid levels and glucose metabolism were analyzed in NC-fed and HFD-fed EC $Fto^{fl/fl}$ and EC $Fto^{\Delta/\Delta}$ mice. Analysis of total triglyceride (Online Figure IV), total cholesterol (Online Figure IV) and low density lipoprotein (LDL; Online Figure IV) revealed no difference between EC $Fto^{fl/fl}$ and EC $Fto^{\Delta/\Delta}$ mice after NC or HFD feeding. High density lipoprotein (HDL), ratios of LDL/HDL, and total cholesterol/HDL were also not influenced by loss of endothelial FTO (Online Figure IV). Conversely, glucose tolerance, as measured by glucose tolerance test (GTT), was significantly improved in HFD-fed EC $Fto^{\Delta/\Delta}$ mice compared to HFD-fed EC $Fto^{fl/fl}$ controls (Figure 2A–B) and fasting blood glucose levels were significantly reduced in HFD-fed EC $Fto^{\Delta/\Delta}$ mice compared to HFD-fed EC $Fto^{fl/fl}$ mice (Online Figure V). In line with these observations, the loss of endothelial FTO significantly reduced serum glycated hemoglobin (Hba1c) levels in HFD-fed mice (HFD: EC $Fto^{fl/fl}$ 6.6%; EC $Fto^{\Delta/\Delta}$ 4.6%) (Figure 2C). Further, loss of endothelial FTO protected against the HFD-induced development of insulin resistance (Figure 2D–E) and hyperinsulinemia (Figure 2F). We could observe no difference in brown adipose tissue function by cold-challenge (Online

Figure V) or on mitochondrial function by *FTO* knockdown in ECs (Online Figure V). *In vivo* insulin stimulation revealed that HFD-feeding reduced AKT phosphorylation at S473 (p-AKT S473) in skeletal muscle, but that AKT phosphorylation was still evident in EC $Fto^{\Delta/\Delta}$ mice (Figure 5G); Further, this effect was also seen *in vitro* (Online Figure V). Taken together, HFD-fed mice lacking FTO in the endothelium are hyperlipidemic similar to controls, but are protected against changes of other key metabolic parameters, chiefly the capacity to respond to insulin.

Loss of endothelial FTO protects from obesity-induced alterations in vascular resistance and hypertension.

To investigate if loss of endothelial FTO not only improves obesity-induced metabolic changes, but also has protective effects on the development of hypertension, blood pressure was analyzed in NC-fed and HFD-fed EC $Fto^{fl/fl}$ and EC $Fto^{\Delta/\Delta}$ mice using radiotelemetry. Although the baseline blood pressure was not altered in NC-fed EC $Fto^{\Delta/\Delta}$ mice, loss of endothelial FTO protected against HFD-induced development of hypertension (Figure 3A) and increases in heart rate (Figure 3B). Since pressure-induced constriction of resistance arteries, which is defined as myogenic tone, is a major determinant of vascular resistance and blood pressure, myogenic tone was analyzed in third order mesenteric arteries of NC-fed and HFD-fed EC $Fto^{fl/fl}$ and EC $Fto^{\Delta/\Delta}$ mice. Similar to blood pressure measurements in NC-fed mice, no difference in myogenic tone was observed between arteries of NC-fed EC $Fto^{fl/fl}$ and EC $Fto^{\Delta/\Delta}$ mice (Figure 3C). However, myogenic tone was protected from HFD-induced decreases in arteries from EC $Fto^{\Delta/\Delta}$ mice, but not from EC $Fto^{fl/fl}$ mice (Figure 3D) suggesting that the loss of endothelial FTO has protective effects on vascular resistance. Further analysis of active (Figure 3E–F) and passive luminal diameters (Figure 3G–H) revealed that HFD-feeding impaired pressure-induced constriction and not stiffness of the arteries and that the loss of endothelial FTO antagonized this development. There was no effect of tamoxifen on these responses (Online Figure VI).

As EDH is a regulator of myogenic tone in resistance arteries, vasoactive response to the IK_{Ca} and SK_{Ca} channel activator NS309 (1 μmol/L), and barium chloride (30 μmol/L), which inhibits K_{ir} channel function, were assessed and found not to be altered (Online Figure VI). Also, smooth muscle depolarization using potassium chloride (40 mM) demonstrated no differences between genotypes (Online Figure VI), and neither was endothelial-dependent vasodilation using acetylcholine (Ach) (Online Figure VII). However, loss of endothelial FTO preserved the vasodilatory response to insulin under HFD conditions (Online Figure VII), an observation in line with data from Figure 2D–E showing also a preserved insulin sensitivity in glucose homeostasis. These data suggest that the loss of endothelial FTO protects from HFD-induced hypertension and preserves myogenic tone and insulin-sensitivity in resistance arteries independent of EDH, responses to Ach (e.g., nitric oxide), or dysfunction of smooth muscle contraction.

Endothelial FTO regulates prostaglandin D_2 levels in mouse and human arteries.

In order to identify candidate signaling pathways that may be involved in FTO-dependent metabolic and vascular effects, DNA microarrays of thoracic aortae of $Fto^{+/+}$ and $Fto^{-/-}$ mice were performed and 32 transcripts identified, which showed more than 3-fold change

in expression by FTO deficiency (Online Table III). Interestingly, these data revealed that the *Lipocalin-type prostaglandin D synthase* (*L-Pgds*), which is known to be important in glucose metabolism and regulation of vascular resistance[17, 19], was 4.4-fold upregulated by FTO deficiency. The upregulation of *L-Pgds* in thoracic aortae was verified using qRT-PCR showing a 10-fold increase of transcript expression in *Fto*-deficient mice (Online Figure VIII). Further analysis of protein lysates from third order mesenteric arteries verified that L-PGDS protein was also significantly upregulated in HFD-fed EC $Fto^{\Delta/\Delta}$ mice compared to EC $Fto^{fl/fl}$ mice (Figure 4A). Because L-PGDS converts prostaglandin H_2 to prostaglandin D_2 (PGD_2), we measured PGD_2 levels and found they were significantly upregulated in both NC-fed and HFD-fed EC $Fto^{\Delta/\Delta}$ mice compared to their respective control (NC: EC $Fto^{fl/fl}$ 2.3 ng/mL and EC $Fto^{\Delta/\Delta}$ 4.1 ng/mL; HFD: EC $Fto^{fl/fl}$ 1.1 ng/mL and EC $Fto^{\Delta/\Delta}$ 6.6 ng/mL) (Figure 4B). To further verify that increased PGD_2 levels mediate effects of endothelial FTO deficiency on myogenic tone, third order mesenteric arteries were isolated from HFD-fed EC $Fto^{fl/fl}$ mice and PGD_2 was applied. PGD_2 increased myogenic tone in vessels of HFD-fed EC $Fto^{fl/fl}$ mice to levels of HFD-fed EC $Fto^{\Delta/\Delta}$ mice (Figure 4C), in effect rescuing the artery from the effects of HFD. In accordance with myogenic tone data from HFD-fed EC $Fto^{\Delta/\Delta}$ mice, PGD_2 addition restored pressure-induced contractility to levels of arteries from NC-fed mice, without influencing overall arterial stiffness (i.e., passive tone; Figure 4D–E). Conversely, when PGD_2 synthesis was inhibited by inhibiting L-PGDS using 10 μM AT-56, the myogenic tone in HFD-fed EC $Fto^{\Delta/\Delta}$ mimicked the myogenic tone from HFD-fed EC $Fto^{fl/fl}$ (Figure 4F) with affecting only the active, but not the passive diameter (Figure 4G–H). Further, the addition of PGD_2 significantly increased AKT phosphorylation in primary cultures of human endothelial cells (Online Figure VIII). Also, global deletion of *L-Pgds* had no additional pathological changes on blood pressure or myogenic tone in presence of HFD-feeding (Online Figure IX).

Last, human arteries from obese or healthy individuals were tested for *FTO* mRNA expression, which was found to be significantly increased in obese arteries (Figure 5A). After incubation of arteries from obese individuals with FTO inhibitors rhein or FB23–2, myogenic tone increased (Figure 5B). The myogenic tone from obese human arteries also increased after direct addition of PGD_2 (Figure 5C). When summed, data from mouse and human suggest that obesity increases FTO expression, which acts to decrease L-PGDS and reduces PGD_2 levels in resistance arteries, with subsequent decreases in insulin tolerance and myogenic tone/ blood pressure. Reversing these effects (e.g., with FTO pharmacological inhibition/ genetic deletion or addition of PGD_2) provided protective effects on both obesity-induced metabolic and vascular changes (Figure 5D).

DISCUSSION

The detrimental effects of obesity-induced metabolic and vascular changes are well known[2, 3, 5]. However, little is known about the role of different cell types in the chronological progression of obesity-induced alterations favoring the deadly effects of obesity, especially of CVDs. Here, we could demonstrate that the loss of endothelial FTO protected from obesity-induced insulin resistance, hyperglycemia and hypertension in presence of adipose tissue inflammation and obesity. These data demonstrate that FTO has a previously unknown function in the vasculature and in the ontogeny of obesity-induced

hypertension. Also, it identifies endothelial FTO as an important regulator in obesity-induced metabolic alterations, which is independent from its known effect on obesity[8]. In addition, our data signify that ECs and specifically endothelial FTO are key mediators in the progression from adipose tissue inflammation to subsequent metabolic and vascular alterations.

We could validate that loss of endothelial FTO did not influence HFD-induced obesity, subsequent inflammation of adipose tissue and the development of dyslipidemia. However, endothelial FTO deletion was protective against the subsequent development of hyperglycemia, hyperinsulinemia, and insulin resistance suggesting that loss of endothelial FTO allowed to maintain physiological EC function under pathologically obese conditions. Indeed, previous studies could clearly show that insulin movement across the EC is vital for maintaining insulin sensitivity[26]. In detail, maintenance of insulin sensitivity of ECs had a protective effect on insulin resistance by specifically preserving skeletal muscle insulin sensitivity, even in presence of dyslipidemia[13, 18]. Mechanistically, this was dependent on HFD-induced impairment of insulin-dependent AKT and eNOS phosphorylation in EC leading to reduced interstitial insulin concentration and glucose uptake of skeletal muscle[13]. Furthermore, this study showed that decreased AKT and eNOS phosphorylation in EC was sufficient to impair glucose and insulin tolerance in mice and that restoration of this pathway reversed the metabolic consequences[13]. These data stress the importance of AKT and eNOS signaling within EC to maintain physiological barrier function to subsequent organs. Interestingly, we could prove that knockdown of *FTO* did not influence mitochondrial function, but increased insulin-induced AKT phosphorylation in EC and skeletal muscle in HFD conditions. These data suggest that loss of endothelial FTO protects from HFD-induced insulin resistance and hyperglycemia by antagonizing decreased AKT phosphorylation in EC and subsequently in skeletal muscle in obese conditions.

Because FTO is a m6A RNA-demethylase and this RNA modification is known to affect mRNA stability, we analyzed which transcripts were altered in expression to identify mediators of FTO-dependent effects[12, 27]. Interestingly, we found that *L-Pgds*, which is known to be m6A-methylated[28], was upregulated by FTO deficiency on mRNA and protein level. L-PGDS is expressed in EC and a known metabolic and vascular effector by synthesizing PGD_2[17, 19, 29],. The loss of endothelial FTO significantly increased PGD_2 levels in the vasculature, thus preventing from HFD-induced decrease. Furthermore, we could reveal that PGD_2 stimulation significantly increased AKT phosphorylation in EC suggesting that increased PGD_2 levels mediate metabolic effects by the loss of endothelial FTO. In line with our finding, a previous report showed that *L-Pgds* deficiency in mice significantly impaired glucose and insulin tolerance[19] and vice versa, that increased PGD_2 levels improved insulin sensitivity in HFD-fed mice[30]. Collectively, our data suggest that increased PGD_2 levels allow maintaining insulin sensitivity under obese conditions by increasing AKT phosphorylation.

In addition to a metabolic function of endothelial FTO, we demonstrate that loss of endothelial FTO protected from HFD-induced hypertension and increases in heart rate. Additional analysis of vascular reactivity in resistance arteries identified that loss of endothelial FTO did not affect depolarization-induced contractility, EDH signaling or Ach-

induced vasodilation. However, it protected from HFD-induced decreases in myogenic tone by preserving pressure-induced contraction. This observation correlating reduced myogenic tone with increased blood pressure in obese and diabetic conditions has also been described in resistance arteries of human, mice and rats and is thought to develop with progression of hypertension as a failure of regulatory mechanism to protect subsequent organs from flow-induced injury[31–37]. Interestingly, we could show that the addition of PGD_2 rescued myogenic tone in resistance arteries of HFD-fed mice and vice versa that inhibiting the PGD_2-synthase L-PGDS reduced myogenic tone in resistance arteries of HFD-fed endothelial FTO-deficient mice, suggesting PGD_2 as a mediator of FTO in regulation of vascular resistance. Collectively, our data suggest that loss of endothelial FTO preserved myogenic tone in resistance arteries by increasing L-PGDS expression and PGD_2 levels, respectively, contributing to the protection from obesity-induced hypertension. Experiments using human obese arteries could demonstrate vasoactive effects in accordance to murine data, as myogenic tone was rescued by either FTO inhibition or PGD_2.

This work identifies endothelial FTO as an important regulator of obesity-induced hyperglycemia, insulin resistance, and hypertension in the presence of obesity and dyslipidemia in mice. Interestingly, even with the protective CVD effects of FTO deletion from endothelium, the mice were still obese and were dyslipidemic. Based on the data presented herein, it is possible FTO and/or L-PGDS could present as a novel drug target to protect from metabolic and vascular risk factors in the setting of obesity and subsequent CVDs.

Supplementary Material

Refer to Web version on PubMed Central for supplementary material.

ACKNOWLEDGEMENTS

We would like to thank the Research Histology Core (University of Virginia School of Medicine) for their help in embedding and cutting of tissues, the Clinical Pathology (University of Virginia School of Medicine) for performing the blood lipid analysis/ELISA. We also thank Prof. Ulrich Rüther (Heinrich-Heine-University Düsseldorf) for his extensive intellectual input. DNA microarray processing and differential expression analysis were performed at the Genomics & Transcriptomics Laboratory of the BMFZ (Heinrich-Heine-University Düsseldorf) by René Deenen und Karl Köhrer.

SOURCES OF FUNDING

Funded by DFG IRTG 1902 (N.K. and A.G.), NIH 088554 (B.E.I.), and the Robert M. Berne Cardiovascular Research Center, University of Virginia School of Medicine.

Nonstandard Abbreviation and Acronyms:

Ach	Acetylcholine
CVD	Cardiovascular disease
EDH	Endothelial-derived hyperpolarization
FTO	Fat mass and obesity associated gene
GTT	Glucose tolerance test

GWAS	Genome-wide association study
HAoEC	Human aortic endothelial cells
Hba1c	Glycated hemoglobin
HDL	High-density lipoprotein
HFD	High fat diet
IK_{Ca}	Intermediate Ca^{2+} -activated potassium channel
IRX3	Iroquois homeobox 3
ITT	Insulin tolerance test
K_{ir}	Inward rectifier potassium channels
LD	Lumen diameter
LDL	Low-density lipoprotein
L-PGDS	Lipocalin-type prostaglandin D synthase
NC	Normal chow
PGD_2	Prostaglandin D_2
SK_{Ca}	Small Ca^{2+} -activated potassium channel
SMC	Smooth muscle cell
SNP	Single nucleotide polymorphism

REFERENCES

1. Bastien M, Poirier P, Lemieux I, Despres JP. Overview of epidemiology and contribution of obesity to cardiovascular disease. Prog Cardiovasc Dis. 2014;56:369–381 [PubMed: 24438728]
2. Xia JY, Holland WL, Kusminski CM, Sun K, Sharma AX, Pearson MJ, Sifuentes AJ, McDonald JG, Gordillo R, Scherer PE. Targeted induction of ceramide degradation leads to improved systemic metabolism and reduced hepatic steatosis. Cell Metab. 2015;22:266–278 [PubMed: 26190650]
3. Li Y, Xu S, Mihaylova MM, Zheng B, Hou X, Jiang B, Park O, Luo Z, Lefai E, Shyy JY, Gao B, Wierzbicki M, Verbeuren TJ, Shaw RJ, Cohen RA, Zang M. Ampk phosphorylates and inhibits srebp activity to attenuate hepatic steatosis and atherosclerosis in diet-induced insulin-resistant mice. Cell Metab. 2011;13:376–388 [PubMed: 21459323]
4. Kubota T, Kubota N, Kadowaki T. Imbalanced insulin actions in obesity and type 2 diabetes: Key mouse models of insulin signaling pathway. Cell Metab. 2017;25:797–810 [PubMed: 28380373]
5. Landsberg L, Aronne LJ, Beilin LJ, Burke V, Igel LI, Lloyd-Jones D, Sowers J. Obesity-related hypertension: Pathogenesis, cardiovascular risk, and treatment--a position paper of the the obesity society and the american society of hypertension. Obesity (Silver Spring). 2013;21:8–24 [PubMed: 23401272]
6. Karaca U, Schram MT, Houben AJ, Muris DM, Stehouwer CD. Microvascular dysfunction as a link between obesity, insulin resistance and hypertension. Diabetes Res Clin Pract. 2014;103:382–387 [PubMed: 24438874]
7. Frayling TM, Timpson NJ, Weedon MN, Zeggini E, Freathy RM, Lindgren CM, Perry JR, Elliott KS, Lango H, Rayner NW, Shields B, Harries LW, Barrett JC, Ellard S, Groves CJ, Knight B, Patch

AM, Ness AR, Ebrahim S, Lawlor DA, Ring SM, Ben-Shlomo Y, Jarvelin MR, Sovio U, Bennett AJ, Melzer D, Ferrucci L, Loos RJ, Barroso I, Wareham NJ, Karpe F, Owen KR, Cardon LR, Walker M, Hitman GA, Palmer CN, Doney AS, Morris AD, Smith GD, Hattersley AT, McCarthy MI. A common variant in the fto gene is associated with body mass index and predisposes to childhood and adult obesity. Science. 2007;316:889–894 [PubMed: 17434869]

8. Fischer J, Koch L, Emmerling C, Vierkotten J, Peters T, Bruning JC, Ruther U. Inactivation of the fto gene protects from obesity. Nature. 2009;458:894–898 [PubMed: 19234441]
9. Smemo S, Tena JJ, Kim KH, Gamazon ER, Sakabe NJ, Gomez-Marin C, Aneas I, Credidio FL, Sobreira DR, Wasserman NF, Lee JH, Puviindran V, Tam D, Shen M, Son JE, Vakili NA, Sung HK, Naranjo S, Acemel RD, Manzanares M, Nagy A, Cox NJ, Hui CC, Gomez-Skarmeta JL, Nobrega MA. Obesity-associated variants within fto form long-range functional connections with irx3. Nature. 2014;507:371–375 [PubMed: 24646999]
10. Berulava T, Horsthemke B. The obesity-associated snps in intron 1 of the fto gene affect primary transcript levels. Eur J Hum Genet. 2010;18:1054–1056 [PubMed: 20512162]
11. Ikels K, Kuschel S, Fischer J, Kaisers W, Eberhard D, Ruther U. Fto is a relevant factor for the development of the metabolic syndrome in mice. PLoS One. 2014;9:e105349 [PubMed: 25144618]
12. Jia G, Fu Y, Zhao X, Dai Q, Zheng G, Yang Y, Yi C, Lindahl T, Pan T, Yang YG, He C. N6-methyladenosine in nuclear rna is a major substrate of the obesity-associated fto. Nat Chem Biol. 2011;7:885–887 [PubMed: 22002720]
13. Kubota T, Kubota N, Kumagai H, Yamaguchi S, Kozono H, Takahashi T, Inoue M, Itoh S, Takamoto I, Sasako T, Kumagai K, Kawai T, Hashimoto S, Kobayashi T, Sato M, Tokuyama K, Nishimura S, Tsunoda M, Ide T, Murakami K, Yamazaki T, Ezaki O, Kawamura K, Masuda H, Moroi M, Sugi K, Oike Y, Shimokawa H, Yanagihara N, Tsutsui M, Terauchi Y, Tobe K, Nagai R, Kamata K, Inoue K, Kodama T, Ueki K, Kadowaki T. Impaired insulin signaling in endothelial cells reduces insulin-induced glucose uptake by skeletal muscle. Cell Metab. 2011;13:294–307 [PubMed: 21356519]
14. Billaud M, Lohman AW, Johnstone SR, Biwer LA, Mutchler S, Isakson BE. Regulation of cellular communication by signaling microdomains in the blood vessel wall. Pharmacol Rev. 2014;66:513–569 [PubMed: 24671377]
15. Sonkusare SK, Dalsgaard T, Bonev AD, Nelson MT. Inward rectifier potassium (kir2.1) channels as end-stage boosters of endothelium-dependent vasodilators. J Physiol. 2016;594:3271–3285 [PubMed: 26840527]
16. Zhao Y, Vanhoutte PM, Leung SW. Vascular nitric oxide: Beyond enos. J Pharmacol Sci. 2015;129:83–94 [PubMed: 26499181]
17. Feletou M, Huang Y, Vanhoutte PM. Endothelium-mediated control of vascular tone: Cox-1 and cox-2 products. Br J Pharmacol. 2011;164:894–912 [PubMed: 21323907]
18. Kanda T, Brown JD, Orasanu G, Vogel S, Gonzalez FJ, Sartoretto J, Michel T, Plutzky J. Ppargamma in the endothelium regulates metabolic responses to high-fat diet in mice. J Clin Invest. 2009;119:110–124 [PubMed: 19065047]
19. Ragolia L, Palaia T, Hall CE, Maesaka JK, Eguchi N, Urade Y. Accelerated glucose intolerance, nephropathy, and atherosclerosis in prostaglandin d2 synthase knock-out mice. J Biol Chem. 2005;280:29946–29955 [PubMed: 15970590]
20. Straub AC, Butcher JT, Billaud M, Mutchler SM, Artamonov MV, Nguyen AT, Johnson T, Best AK, Miller MP, Palmer LA, Columbus L, Somlyo AV, Le TH, Isakson BE. Hemoglobin alpha/enos coupling at myoendothelial junctions is required for nitric oxide scavenging during vasoconstriction. Arterioscler Thromb Vasc Biol. 2014;34:2594–2600 [PubMed: 25278292]
21. Billaud M, Lohman AW, Straub AC, Parpaite T, Johnstone SR, Isakson BE. Characterization of the thoracodorsal artery: Morphology and reactivity. Microcirculation. 2012;19:360–372 [PubMed: 22335567]
22. Kumar A, Harris TE, Keller SR, Choi KM, Magnuson MA, Lawrence JC, Jr. Muscle-specific deletion of rictor impairs insulin-stimulated glucose transport and enhances basal glycogen synthase activity. Mol Cell Biol. 2008;28:61–70 [PubMed: 17967879]

23. Kenwood BM, Weaver JL, Bajwa A, Poon IK, Byrne FL, Murrow BA, Calderone JA, Huang L, Divakaruni AS, Tomsig JL, Okabe K, Lo RH, Cameron Coleman G, Columbus L, Yan Z, Saucerman JJ, Smith JS, Holmes JW, Lynch KR, Ravichandran KS, Uchiyama S, Santos WL, Rogers GW, Okusa MD, Bayliss DA, Hoehn KL. Identification of a novel mitochondrial uncoupler that does not depolarize the plasma membrane. Mol Metab. 2014;3:114–123 [PubMed: 24634817]
24. Shu X, Ruddiman CA, Keller TCSt, Keller AS, Yang Y, Good ME, Best AK, Columbus L, Isakson BE. Heterocellular contact can dictate arterial function. Circ Res. 2019;124:1473–1481 [PubMed: 30900949]
25. Alberti KG, Eckel RH, Grundy SM, Zimmet PZ, Cleeman JI, Donato KA, Fruchart JC, James WP, Loria CM, Smith SC Jr., International Diabetes Federation Task Force on E, Prevention, Hational Heart L, Blood I, American Heart A, World Heart F, International Atherosclerosis S, International Association for the Study of O. Harmonizing the metabolic syndrome: A joint interim statement of the international diabetes federation task force on epidemiology and prevention; national heart, lung, and blood institute; american heart association; world heart federation; international atherosclerosis society; and international association for the study of obesity. Circulation. 2009;120:1640–1645 [PubMed: 19805654]
26. Barrett EJ, Liu Z. The endothelial cell: An “early responder” in the development of insulin resistance. Rev Endocr Metab Disord. 2013;14:21–27 [PubMed: 23306779]
27. Wang X, Lu Z, Gomez A, Hon GC, Yue Y, Han D, Fu Y, Parisien M, Dai Q, Jia G, Ren B, Pan T, He C. N6-methyladenosine-dependent regulation of messenger rna stability. Nature. 2014;505:117–120 [PubMed: 24284625]
28. Dominissini D, Moshitch-Moshkovitz S, Schwartz S, Salmon-Divon M, Ungar L, Osenberg S, Cesarkas K, Jacob-Hirsch J, Amariglio N, Kupiec M, Sorek R, Rechavi G. Topology of the human and mouse m6a rna methylomes revealed by m6a-seq. Nature. 2012;485:201–206 [PubMed: 22575960]
29. Taba Y, Sasaguri T, Miyagi M, Abumiya T, Miwa Y, Ikeda T, Mitsumata M. Fluid shear stress induces lipocalin-type prostaglandin d(2) synthase expression in vascular endothelial cells. Circ Res. 2000;86:967–973 [PubMed: 10807869]
30. Fujitani Y, Aritake K, Kanaoka Y, Goto T, Takahashi N, Fujimori K, Kawada T. Pronounced adipogenesis and increased insulin sensitivity caused by overproduction of prostaglandin d2 in vivo. FEBS J. 2010;277:1410–1419 [PubMed: 20136655]
31. Schofield I, Malik R, Izzard A, Austin C, Heagerty A. Vascular structural and functional changes in type 2 diabetes mellitus: Evidence for the roles of abnormal myogenic responsiveness and dyslipidemia. Circulation. 2002;106:3037–3043 [PubMed: 12473548]
32. Ogalla E, Claro C, Alvarez de Sotomayor M, Herrera MD, Rodriguez-Rodriguez R. Structural, mechanical and myogenic properties of small mesenteric arteries from apoe ko mice: Characterization and effects of virgin olive oil diets. Atherosclerosis. 2015;238:55–63 [PubMed: 25437891]
33. Sweazea KL, Walker BR. Impaired myogenic tone in mesenteric arteries from overweight rats. Nutr Metab (Lond). 2012;9:18 [PubMed: 22424473]
34. Ito I, Jarajapu YP, Guberski DL, Grant MB, Knot HJ. Myogenic tone and reactivity of rat ophthalmic artery in acute exposure to high glucose and in a type ii diabetic model. Invest Ophthalmol Vis Sci. 2006;47:683–692 [PubMed: 16431968]
35. Sachidanandam K, Hutchinson JR, Elgebaly MM, Mezzetti EM, Wang MH, Ergul A. Differential effects of diet-induced dyslipidemia and hyperglycemia on mesenteric resistance artery structure and function in type 2 diabetes. J Pharmacol Exp Ther. 2009;328:123–130 [PubMed: 18941121]
36. Thompson JA, Larion S, Mintz JD, Belin de Chantemele EJ, Fulton DJ, Stepp DW. Genetic deletion of nadph oxidase 1 rescues microvascular function in mice with metabolic disease. Circ Res. 2017;121:502–511 [PubMed: 28684629]
37. Tecilazich F, Feke GT, Mazzantini S, Sobrin L, Lorenzi M. Defective myogenic response of retinal vessels is associated with accelerated onset of retinopathy in type 1 diabetic individuals. Invest Ophthalmol Vis Sci. 2016;57:1523–1529 [PubMed: 27035625]

NOVELTY AND SIGNIFICANCE

What Is Known?

- The Fat mass and obesity associated gene *FTO* gene has been associated with obesity.
- Endothelial dysfunction is a hallmark of obesity-associated cardiovascular diseases.
- Myogenic tone, blood pressure, and insulin sensitivity are severely altered in obesity.

What New Information Does This Article Contribute?

- Obesity increases FTO expression in vascular tissue in mouse and human.
- Selective deletion of FTO from endothelium in mice results in preservation of myogenic tone, blood pressure, and insulin sensitivity only in high fat diet-induced obese animals.
- In endothelium, FTO regulates L-PGDS transcript and protein expression, thereby determining the amount of PGD_2 that is present in the vasculature and altering myogenic tone and insulin sensitivity.
- Human arteries have improved myogenic tone in response to FTO inhibition or addition of PGD_2.

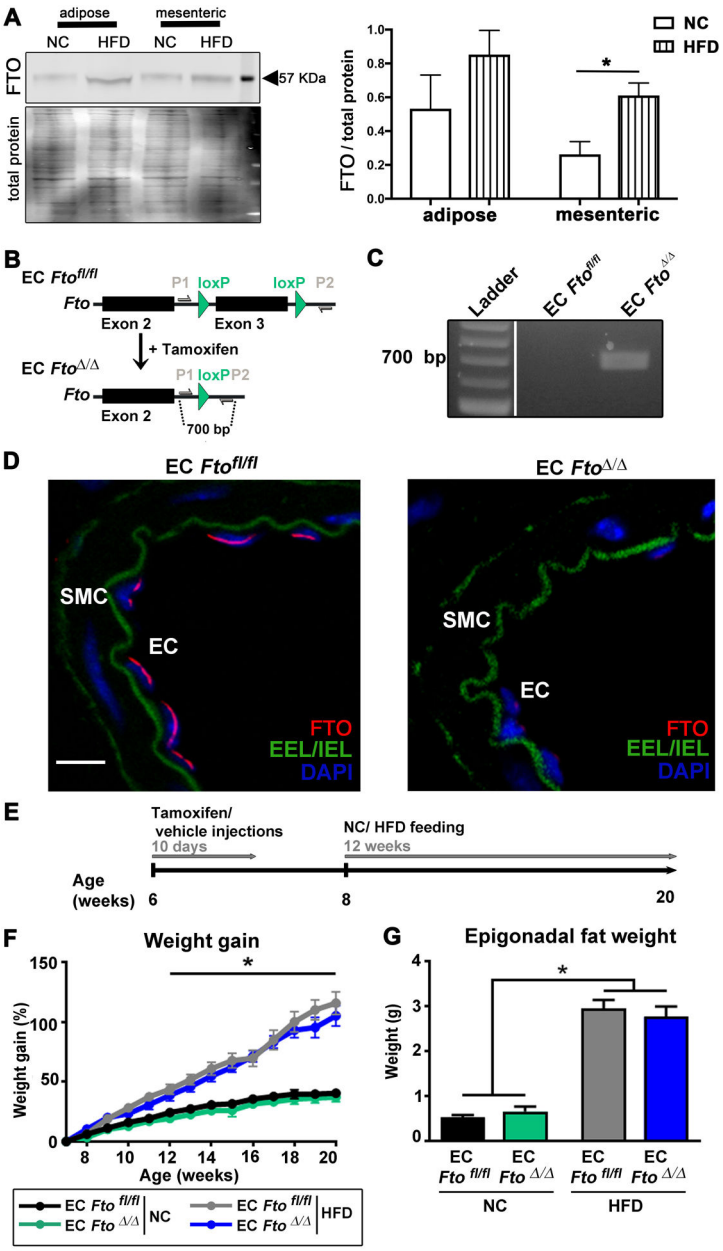

Figure 1: Loss of endothelial FTO did not affect the development of obesity.

(A) Representative western blot and quantification for FTO and total protein expression are shown for lysates of adipose and mesenteric arteries isolated from NC-fed and HFD-fed 20 week old C57BL6 mice (n=3 mice) (*P=0.036 mesenteric NC vs. HFD; n.s. for adipose NC vs. HFD). The image was chosen to present the respective mean value. (B) Schematic illustration of the floxed *Fto* locus (EC $Fto^{fl/fl}$). Administration of tamoxifen resulted in cre-mediated deletion of exon 3 in the *Fto* gene of endothelial cells (EC $Fto^{\Delta/\Delta}$). (C) PCR analysis of *Fto* exon 3 deletion in the heart from EC $Fto^{\Delta/\Delta}$ and EC $Fto^{fl/fl}$ mice. (D) Immunofluorescence of FTO protein (red), cell nuclei (DAPI, blue) as well as inner and outer elastic laminae (IEL, EEL; autofluorescence, green) in third order mesenteric arteries isolated from EC $Fto^{fl/fl}$ and EC $Fto^{\Delta/\Delta}$ mice. Scale bar is 5 μm for both images. (E)

Experimental design for tamoxifen injections and induction of obesity. The 6 week old mice were injected with either vehicle (EC $Fto^{fl/fl}$), or tamoxifen (EC $Fto^{\Delta/\Delta}$) for 10 days. At 8 weeks, mice were either kept on normal chow (NC; EC $Fto^{fl/fl}$ black bars/lines, EC $Fto^{\Delta/\Delta}$ green bars/lines), or fed a high fat diet (HFD; EC $Fto^{fl/fl}$ grey bars/lines, EC $Fto^{\Delta/\Delta}$ blue bars/lines), for 12 weeks. (F) Measurement of weight gain over time in 7–20 week old NC-fed and HFD-fed EC $Fto^{fl/fl}$ and EC $Fto^{\Delta/\Delta}$ mice (n=8–11; $*P<0.0007$ NC-fed EC $Fto^{fl/fl}$ vs. HFD-fed EC $Fto^{fl/fl}$; $*P<0.0001$ NC-fed EC $Fto^{fl/fl}$ vs. HFD-fed EC $Fto^{\Delta/\Delta}$; $*P<0.0001$ NC-fed EC $Fto^{\Delta/\Delta}$ vs. HFD-fed EC $Fto^{\Delta/\Delta}$; $*P<0.0001$ NC-fed EC $Fto^{\Delta/\Delta}$ vs. HFD-fed EC $Fto^{fl/fl}$ from week 12 to 20; n.s. between genotypes on one chow). (G) Analysis of epigonadal fat mass of 20 week old NC-fed and HFD-fed EC $Fto^{fl/fl}$ and EC $Fto^{\Delta/\Delta}$ mice (n=9–10; $*P<0.0001$ NC-fed EC $Fto^{fl/fl}$ vs. HFD-fed EC $Fto^{fl/fl}$; $*P<0.0001$ NC-fed EC $Fto^{fl/fl}$ vs. HFD-fed EC $Fto^{\Delta/\Delta}$; $*P<0.0001$ NC-fed EC $Fto^{\Delta/\Delta}$ vs. HFD-fed EC $Fto^{\Delta/\Delta}$; $*P<0.0001$ NC-fed EC $Fto^{\Delta/\Delta}$ vs. HFD-fed EC $Fto^{fl/fl}$; n.s. between genotypes on one chow). In this figure, values are means ± SEM. For statistical analysis, t-test was used in A or one way ANOVA (F +G) were performed followed by Tukey's post-hoc test, *p<0.05 was defined as significant.

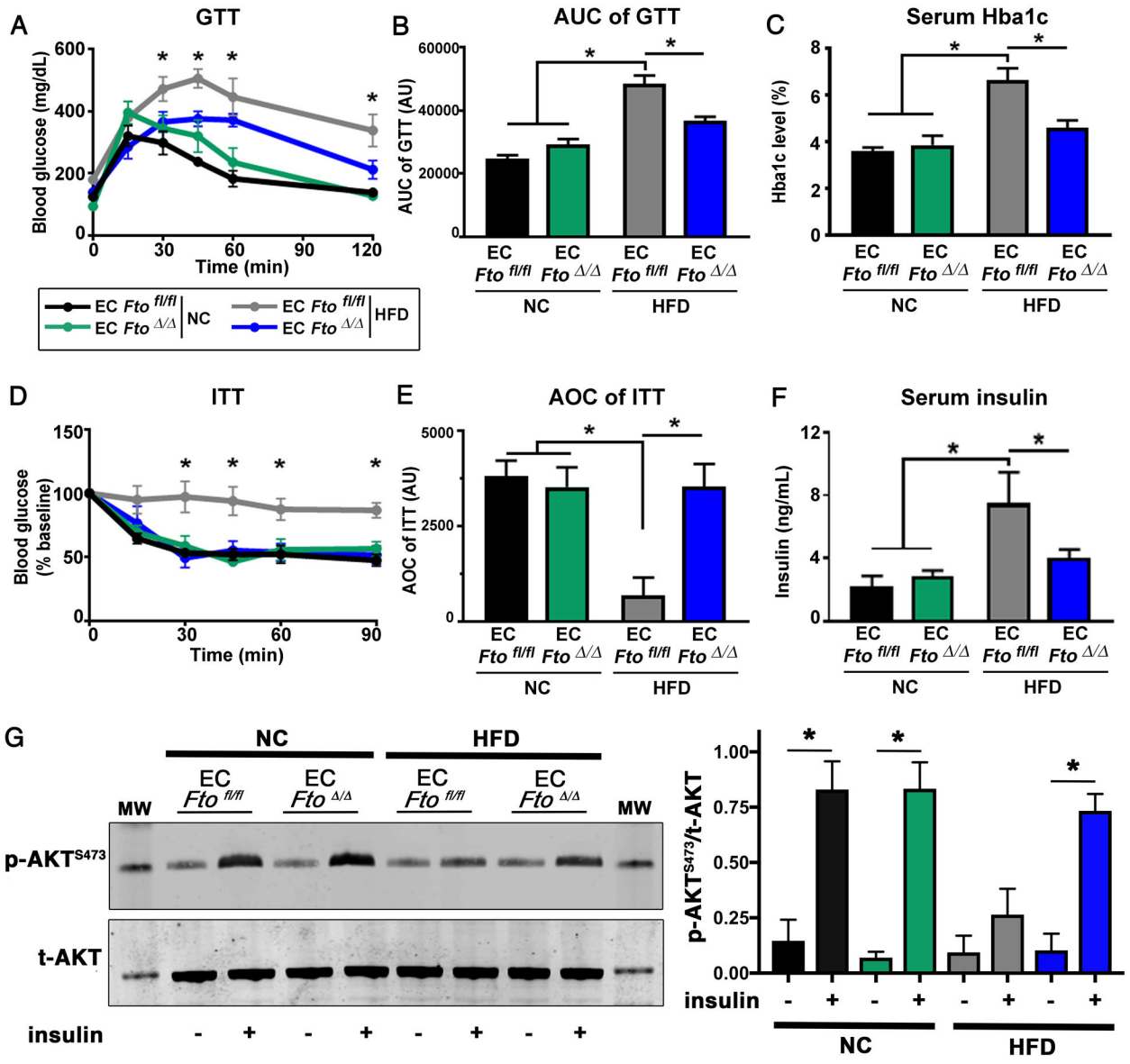

Figure 2: Loss of endothelial FTO specifically improves glucose metabolism in HFD-fed mice.

Experiments were performed in 20 week old NC-fed and HFD-fed EC *Fto*$^{fl/fl}$ and EC *Fto*$^{Δ/Δ}$ mice. Colors for bars and lines: NC-fed EC *Fto*$^{fl/fl}$ black and EC *Fto*$^{Δ/Δ}$ green; HFD-fed EC *Fto*$^{fl/fl}$ grey and EC *Fto*$^{Δ/Δ}$ blue. (A) Glucose tolerance was measured by intraperitoneal (i.p) injection of glucose and (B) the respective area under curve (AUC) determined (n=6–9; **P*<0.0001 NC-fed EC *Fto*$^{fl/fl}$ vs. HFD-fed EC *Fto*$^{fl/fl}$; **P*<0.0001 NC-fed EC *Fto*$^{Δ/Δ}$ vs. HFD-fed EC *Fto*$^{fl/fl}$; **P*=0.0002 HFD-fed EC *Fto*$^{Δ/Δ}$ vs. HFD-fed EC *Fto*$^{fl/fl}$; n.s. NC-fed EC *Fto*$^{Δ/Δ}$ vs. NC-fed EC *Fto*$^{fl/fl}$). (C) Serum Hba1c levels were measured (n=3–7; **P*=0.0011 NC-fed EC *Fto*$^{fl/fl}$ vs. HFD-fed EC *Fto*$^{fl/fl}$; **P*=0.0024 NC-fed EC *Fto*$^{Δ/Δ}$ vs. HFD-fed EC *Fto*$^{fl/fl}$; **P*=0.0060 HFD-fed EC *Fto*$^{Δ/Δ}$ vs. HFD-fed EC *Fto*$^{fl/fl}$; n.s. NC-fed EC *Fto*$^{Δ/Δ}$ vs. NC-fed EC *Fto*$^{fl/fl}$). (D) Insulin tolerance was analyzed after i.p. injection of insulin and (E) the respective AUC calculated (n=3–7; **P*=0.0076 NC-fed EC *Fto*$^{fl/fl}$ vs. HFD-fed EC *Fto*$^{fl/fl}$; **P*=0.0159 NC-fed EC *Fto*$^{Δ/Δ}$ vs. HFD-fed EC *Fto*$^{fl/fl}$; **P*=0.0180

HFD-fed EC *Fto*$^{\Delta/\Delta}$ vs. HFD-fed EC *Fto*$^{fl/fl}$; n.s. NC-fed EC *Fto*$^{\Delta/\Delta}$ vs. NC-fed EC *Fto*$^{fl/fl}$). (F) Measurement of serum insulin levels (n=3–6; **P*=0.0027 NC-fed EC *Fto*$^{fl/fl}$ vs. HFD-fed EC *Fto*$^{fl/fl}$; **P*=0.0058 NC-fed EC *Fto*$^{\Delta/\Delta}$ vs. HFD-fed EC *Fto*$^{fl/fl}$; **P*=0.0410 HFD-fed EC *Fto*$^{\Delta/\Delta}$ vs. HFD-fed EC *Fto*$^{fl/fl}$; n.s. NC-fed EC *Fto*$^{\Delta/\Delta}$ vs. NC-fed EC *Fto*$^{fl/fl}$). (G) Representative western blot and quantification for p-AKT^{S473} and total AKT are shown for lysates isolated from skeletal muscle after in vivo insulin stimulation (n=3; **P*=0.0099 NC-fed EC *Fto*$^{fl/fl}$ with vs. w/o insulin; **P*=0.0053 NC-fed EC *Fto*$^{\Delta/\Delta}$ with vs. w/o insulin; **P*=0.0012 HFD-fed EC *Fto*$^{fl/fl}$ with vs. w/o insulin; n.s. HFD-fed EC *Fto*$^{fl/fl}$ with vs. w/o insulin). The respective western blot was selected to reflect the mean value. Molecular weight marker is 60 kDa. In this figure, values are means ± SEM. For statistical analysis, one way ANOVA were performed followed by Tukey's post-hoc test (A-F); student's t-test was used in G; *p<0.05 was defined as significant.

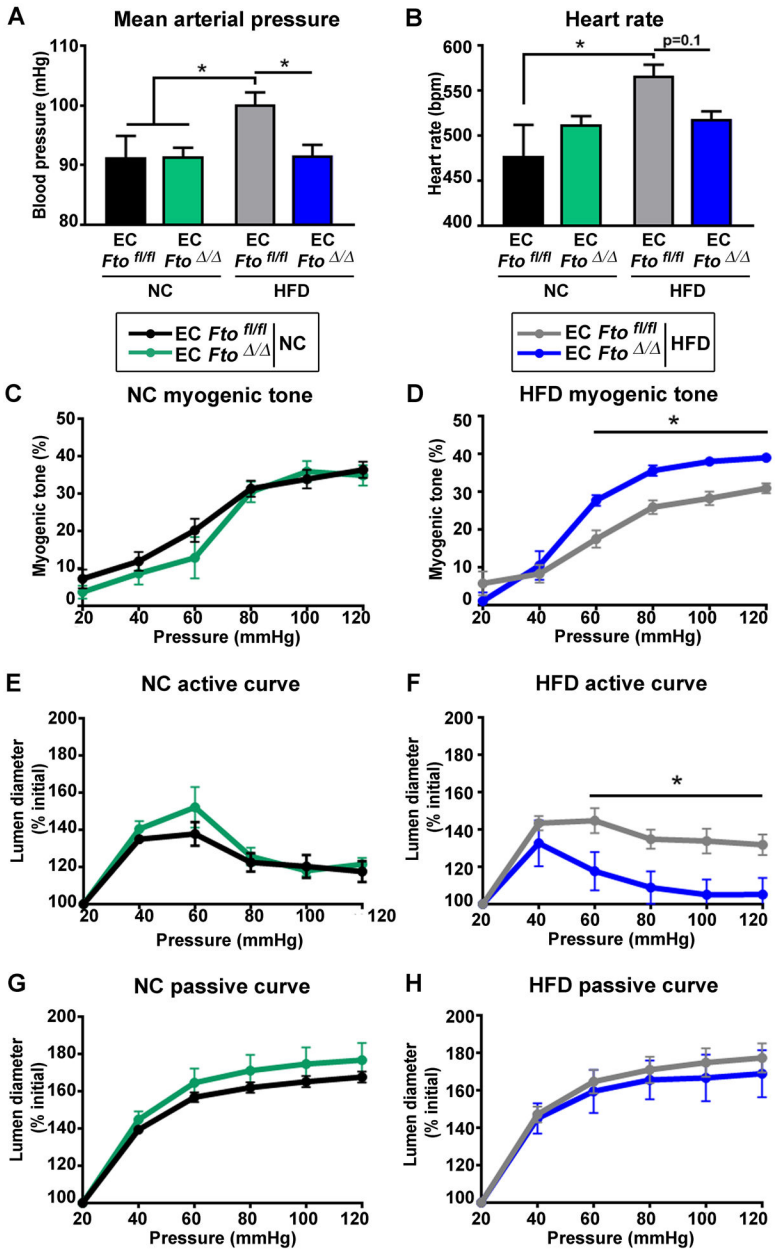

Figure 3: Endothelial FTO deficiency protects from HFD-induced vascular changes and hypertension.

Experiments were performed in 20 week old NC-fed and HFD-fed EC $Fto^{fl/fl}$ and EC $Fto^{\Delta/\Delta}$ mice. Colors for bars and lines: NC-fed EC $Fto^{fl/fl}$ black and EC $Fto^{\Delta/\Delta}$ green; HFD-fed EC $Fto^{fl/fl}$ grey and EC $Fto^{\Delta/\Delta}$ blue. Radiotelemetric analysis of (A) mean arterial pressure and (B) heart rate (n=5–8; For (A): *P=0.0484 NC-fed EC $Fto^{fl/fl}$ vs. HFD-fed EC $Fto^{fl/fl}$; *P=0.0386 NC-fed EC $Fto^{\Delta/\Delta}$ vs. HFD-fed EC $Fto^{fl/fl}$; *P=0.0484 HFD-fed EC $Fto^{\Delta/\Delta}$ vs. HFD-fed EC $Fto^{fl/fl}$; n.s. NC-fed EC $Fto^{\Delta/\Delta}$ vs. NC-fed EC $Fto^{fl/fl}$; For (B): *P=0.0050 NC-fed EC $Fto^{fl/fl}$ vs. HFD-fed EC $Fto^{fl/fl}$; P=0.1070 NC-fed EC $Fto^{\Delta/\Delta}$ vs. HFD-fed EC $Fto^{fl/fl}$; P=0.1016 HFD-fed EC $Fto^{\Delta/\Delta}$ vs. HFD-fed EC $Fto^{fl/fl}$; n.s. NC-fed EC $Fto^{\Delta/\Delta}$ vs. NC-fed EC $Fto^{fl/fl}$). Pressure myograph analysis in third order mesenteric arteries of NC-fed (C, E,

G, left column) and HFD-fed mice (D, F, H, right column). (C-D) Analysis of myogenic tone with respective (E-F) active and (G-H) passive curves (n=4–8; For (C, E, G): NC-fed EC $Fto^{fl/fl}$ vs. NC-fed EC $Fto^{fl/fl}$ n.s. at all pressures; For (D): HFD-fed EC $Fto^{\Delta/\Delta}$ vs. HFD-fed EC $Fto^{fl/fl}$ n.s. at 20 and 40 mmHg, $^{*}P$=0.0422/ 0.056/ 0.050/ 0.0206 at 60/ 80/ 100/ 120 mmHg; For (F): HFD-fed EC $Fto^{\Delta/\Delta}$ vs. HFD-fed EC $Fto^{fl/fl}$ n.s. at 20 and 40 mmHg, $^{*}P$=0.0454/ 0.0322/ 0.0271/ 0.0239 at 60/ 80 / 100/ 120 mmHg; For (H): HFD-fed EC $Fto^{\Delta/\Delta}$ vs. HFD-fed EC $Fto^{fl/fl}$ n.s. at all pressures). In this figure, values are means ± SEM. For statistical analysis, one way ANOVA was performed followed by Tukey's post-hoc test, *p<0.05 was defined as significant.

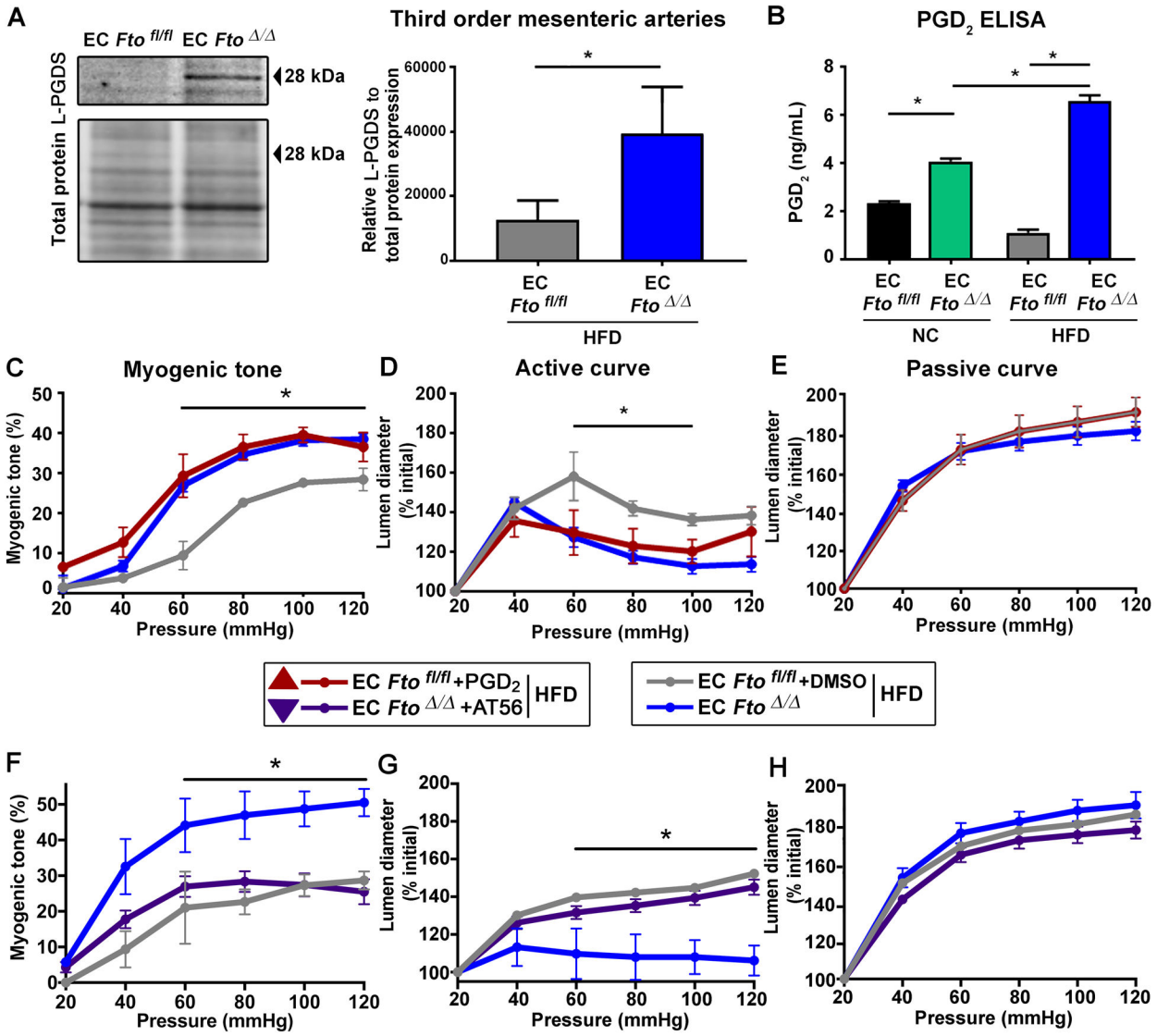

Figure 4: Increased PGD_2 levels can rescue HFD-induced vascular changes.

Experiments were performed in 20 week old NC-fed and HFD-fed EC *Fto*$^{fl/fl}$ and EC *Fto*$^{Δ/Δ}$ mice. Colors for bars and lines: NC-fed EC *Fto*$^{fl/fl}$ black and EC *Fto*$^{Δ/Δ}$ green; HFD-fed EC *Fto*$^{fl/fl}$ grey and EC *Fto*$^{Δ/Δ}$ blue; HFD-fed EC *Fto*$^{fl/fl}$+PGD_2 red and HFD-fed EC *Fto*$^{Δ/Δ}$ +AT56 purple. (A) Representative western blot and quantification for Lipocalin-type Prostaglandin D2 synthase (L-PGDS) relative to total protein staining from protein lysates of third order mesenteric arteries isolated from HFD-fed EC *Fto*$^{fl/fl}$ and EC *Fto*$^{Δ/Δ}$ mice (n=3; **P*=0.041). The image was selected to reflect the respective mean value. (B) PGD_2 ELISA of thoracic aortae isolated from NC-fed and HFD-fed EC *Fto*$^{fl/fl}$ and EC *Fto*$^{Δ/Δ}$ mice (n=3–5; **P*=0.0025 NC-fed EC *Fto*$^{fl/fl}$ vs. HFD-fed EC *Fto*$^{fl/fl}$; **P*<0.0001 NC-fed EC *Fto*$^{Δ/Δ}$ vs. HFD-fed EC *Fto*$^{fl/fl}$; **P*<0.0001 HFD-fed EC *Fto*$^{Δ/Δ}$ vs. HFD-fed EC *Fto*$^{fl/fl}$; **P*<0.0001 NC-fed EC *Fto*$^{Δ/Δ}$ vs. NC-fed EC *Fto*$^{fl/fl}$). (C-E) Pressure myograph analysis in third order mesenteric arteries isolated from HFD-fed EC *Fto*$^{fl/fl}$ mice after addition of PGD_2 or vehicle alone (DMSO) in comparison to vessels of HFD-fed EC *Fto*$^{Δ/Δ}$ mice. Analysis of (C)

myogenic tone and respective (D) active and (E) passive curves (n=3; For (C): HFD-fed EC $Fto^{fl/fl}$ + DMSO vs. HFD-fed EC $Fto^{fl/fl}$ + PGD_2 n.s. at 20 and 40 mmHg, *P=0.0370/ 0.0132/ 0.046/ 0.048 at 60/ 80/ 100/ 120 mmHg; For (D): HFD-fed EC $Fto^{fl/fl}$ + DMSO vs. HFD-fed EC $Fto^{fl/fl}$ + PGD_2 n.s. at 20, 40 and 120 mmHg, *P=0.0410/ 0.0302/ 0.043 at 60/ 80/ 100 mmHg; For (E): HFD-fed EC $Fto^{fl/fl}$ + DMSO vs. HFD-fed EC $Fto^{fl/fl}$ + PGD_2 n.s. at all pressures). (F-H) Pressure myograph analysis in third order mesenteric arteries isolated from EC $Fto^{\Delta/\Delta}$ mice after addition of AT56 or vehicle alone (DMSO) in comparison to vessels of HFD-fed EC $Fto^{fl/fl}$ mice (n=5; For (F): HFD-fed EC $Fto^{\Delta/\Delta}$ mice vs. HFD-fed EC $Fto^{\Delta/\Delta}$ mice + AT-56 n.s. at 20 and 40 mmHg, *P=0.045/ 0.039/ 0.033/ 0.022 at 60/ 80/ 100/ 120 mmHg; For (G): HFD-fed EC $Fto^{\Delta/\Delta}$ mice vs. HFD-fed EC $Fto^{\Delta/\Delta}$ mice + AT-56 n.s. at 20 and 40 mmHg, *P=0.046/ 0.048/ 0.041/ 0.032 at 60/ 80/ 100/ 120 mmHg; For (H): HFD-fed EC $Fto^{\Delta/\Delta}$ mice vs. HFD-fed EC $Fto^{\Delta/\Delta}$ mice + AT-56 n.s. at all pressures). In this figure, values are means ± SEM. For statistical analysis, unpaired students t-test (in A) or one-way ANOVA (in B-H) was performed followed by Tukey's post-hoc test, *p<0.05 was defined as significant.

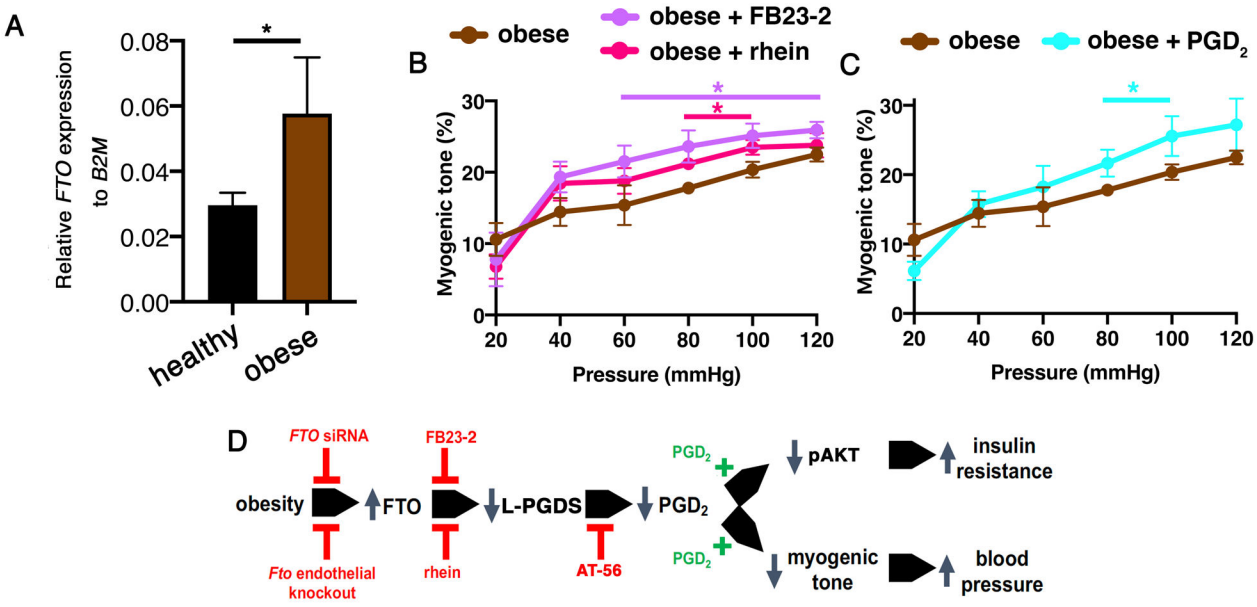

Figure 5: Inhibition of FTO or increased PGD_2-levels can rescue vascular changes in obese humans.

Experiments were performed with adipose arteries isolated from healthy and obese humans (n=3 healthy and n=3 obese). (A) qRT-PCR for *FTO* demonstrates significantly increased *FTO* expression in obese arteries (**P*=0.0400) (B-C) Analysis of myogenic tone in arteries isolated from adipose tissue of obese human in (B) presence of FTO inhibitors rhein and FB23–2 or (C) after addition of PGD_2 (n=3 per condition; For (B): Obese vs. obese + Rhein n.s. at 20–60 and 120 mmHg, **P*=0.025/ 0.048 at 80/ 100 mmHg; Obese vs. obese + FB-23–2 n.s. at 20 and 40 mmHg, **P*=0.041/ 0.038/ 0.042/ 0.047 at 60/ 80/ 100/ 120 mmHg; For (C): Obese vs. obese + PGD_2 n.s. at 20–60 and 120 mmHg, **P*=0.045/ 0.048 at 80/ 100 mmHg). In this figure, values are means ± SEM. For statistical analysis, unpaired students t-test (in A) or one-way ANOVA (in B-C) was performed followed by Tukey's post-hoc test, *p<0.05 was defined as significant. (D) Illustrates a proposed mechanism for FTO's role in endothelium for regulating PGD_2 with downstream pathophysiological outcomes. Red (inhibitory) and green (addition) are at pathway checkpoints that can reverse the proposed etiology.